JACC: CARDIOVASCULAR IMAGING VOL. ■, NO. ■, 2020

CLINICAL RESEARCH

Extracellular Volume and Global Longitudinal Strain Both Associate With Outcomes But Correlate Minimally

Fredrika Fröjdh, MD,[a] Yaron Fridman, MD,[b] Patrick Bering, MD,[c] Aatif Sayeed, MD,[c] Maren Maanja, MD,[a] Louise Niklasson, MD,[a] Eric Olausson, MD,[a] Hongyang Pi, MD,[c] Ali Azeem, MD,[c] Timothy C. Wong, MD, MS,[c,d,e,f] Peter Kellman, PhD,[g] Brian Feingold, MD, MS,[f,h] Adam Christopher, MD,[h] Miho Fukui, MD,[i] João L. Cavalcante, MD,[i] Christopher A. Miller, MBBCh, PhD,[j,k,l] Javed Butler, MD, MPH,[m] Martin Ugander, MD, PhD,[a,n] Erik B. Schelbert, MD, MS[c,d,e,f]

ABSTRACT

OBJECTIVES This study examined how ECV and GLS relate to each other and to outcomes.

BACKGROUND Among myriad changes occurring in diseased myocardium, left ventricular imaging metrics of either the interstitium (e.g., extracellular volume [ECV]) or contractile function (e.g., global longitudinal strain [GLS]) may consistently associate with adverse outcomes yet correlate minimally with each other. This scenario suggests that ECV and GLS potentially represent distinct domains of cardiac vulnerability.

METHODS The study included 1,578 patients referred for cardiovascular magnetic resonance (CMR) without amyloidosis, and it quantified how ECV associated with GLS in linear regression models. ECV and GLS were then compared in their associations with incident outcomes (death and hospitalization for heart failure).

RESULTS ECV and GLS correlated minimally ($R^2 = 0.04$). Over a median follow-up of 5.6 years, 339 patients experienced adverse events (149 hospitalizations for heart failure, 253 deaths, and 63 with both). GLS (univariable hazard ratio: 2.07 per 5% increment; 95% CI: 1.86 to 2.29) and ECV (univariable hazard ratio: 1.66 per 4% increment; 95% CI: 1.51 to 1.82) were principal variables associating with outcomes in univariable and multivariable Cox regression models. Similar results were observed in several clinically important subgroups. In the whole cohort, ECV added prognostic value beyond GLS in univariable and multivariable Cox regression models.

CONCLUSIONS GLS and ECV may represent principal but distinct domains of cardiac vulnerability, perhaps reflecting their distinct cellular origins. Whether combining ECV and GLS may advance pathophysiological understanding for a given patient, optimize risk stratification, and foster personalized medicine by targeted therapeutics requires further investigation. (J Am Coll Cardiol Img 2020;■:■–■) © 2020 the American College of Cardiology Foundation. Published by Elsevier. All rights reserved.

From the [a]Department of Clinical Physiology, Karolinska University Hospital, and Karolinska Institutet, Stockholm, Sweden; [b]Asheville Cardiology Associates, Mission Hospital, Asheville, North Carolina; [c]UPMC Cardiovascular Magnetic Resonance Center, UPMC, Pittsburgh, Pennsylvania; [d]Department of Medicine, University of Pittsburgh School of Medicine, Pittsburgh, Pennsylvania; [e]Heart and Vascular Institute, UPMC, Pittsburgh, Pennsylvania; [f]Clinical and Translational Science Institute, University of Pittsburgh, Pittsburgh, Pennsylvania; [g]National Heart Lung and Blood Institute, Bethesda, Maryland; [h]Department of Pediatrics, University of Pittsburgh School of Medicine, Pittsburgh, Pennsylvania; [i]Minneapolis Heart Institute, Abbott Northwestern Hospital, Minneapolis, Minnesota; [j]Division of Cardiovascular Sciences, School of Medical Sciences, Faculty of Biology, Medicine and Health, Manchester Academic Health Science Centre, University of Manchester, Manchester, United Kingdom; [k]Manchester University NHS Foundation Trust, Wythenshawe, Manchester, United Kingdom; [l]Wellcome Centre for Cell-Matrix Research, Division of Cell-Matrix Biology & Regenerative Medicine, School of Biology, Faculty of Biology, Medicine & Health, Manchester Academic Health Science Centre, University of Manchester, Manchester, United Kingdom; [m]Department of Medicine, University of Mississippi, Jackson, Mississippi; and the [n]Kolling Institute, Royal North Shore Hospital, and Sydney Medical School, Northern Clinical School, University of Sydney, Sydney, Australia. This work was supported by several entities. Dr. Miller is funded by a Clinician Scientist Award (CS-2015-15-003) from the National Institute for Health (NIH) Research. Dr. Wong was supported by an American Heart Association Scientist Development grant and a Children's Cardiomyopathy Foundation grant. Dr. Feingold was supported by an American Heart Association Enduring Hearts grant

ISSN 1936-878X/$36.00 https://doi.org/10.1016/j.jcmg.2020.04.026

ABBREVIATIONS AND ACRONYMS

BNP = B-type natriuretic peptide

CMR = cardiovascular magnetic resonance

DMF = diffuse myocardial fibrosis

ECV = extracellular volume

LVEF = left ventricular ejection fraction

GLS = global longitudinal strain

HHF = hospitalization for heart failure

HR = hazard ratio

IDI = integrated discrimination improvement

LGE = late gadolinium enhancement

MI = myocardial infarction

NRI = net reclassification improvement

Q1 to Q3 = quartile 1 to quartile 3

Among myriad changes occurring in diseased myocardium, diffuse myocardial interstitial expansion and contractile dysfunction may represent principal domains of myocardial disease that remain largely independent of one another, possibly reflecting their distinct origins in the myocardium. For example, cardiovascular magnetic resonance (CMR) extracellular volume (ECV) may reflect architectural distortion, potentially from fibroblast-mediated diffuse myocardial fibrosis (DMF) (1–3), whereas global longitudinal strain (GLS) (4–8) could reflect generalized cardiomyocyte dysfunction, potentially related to abnormal calcium handling, sarcomeric dysfunction, or mitochondrial dysfunction. These GLS and ECV phenotypes might capture fundamental vulnerability prevalent across many ischemic and nonischemic disease states. Ascertaining GLS and ECV phenotypes may inform the mechanistic evaluation of therapeutic responses to interventions and ultimately foster personalized precision medicine through targeted therapeutics.

ECV and GLS metrics seem robust. In the absence of amyloidosis, edema, or inflammation (9), ECV measures excluding focal replacement fibrosis provide a validated metric to quantify DMF (1–3). DMF is a prevalent but potentially reversible (2) derangement in myocardial architecture causing some systolic (10) and especially diastolic (11,12) dysfunction, microvascular dysfunction (13), and electric dysfunction (14) culminating in adverse outcomes (15–21). GLS measurement of left ventricular deformation quantifies changes in systolic function (22) independent of geometric factors (23) through feature tracking, analogous to echocardiographic speckle tracking (4,5). GLS offers ease of measurement, good intraobserver and interobserver reproducibility (24), and robust risk stratification (4–8). Even when left ventricular ejection fraction (LVEF) is normal, both ECV and GLS detect left ventricular disease (2,11,12,22) and stratify risk (2,6,22).

The current study included a large sample of patients referred to a single CMR center serving an integrated health system to examine relationships between ECV, GLS, and outcomes. We hypothesized that ECV and GLS would correlate minimally yet each associate with incident death or hospitalization for heart failure (HHF). We also examined several subgroups, including those with and without preserved LVEF, heart failure, diabetes, myocardial infarction (MI), or evident coronary disease, hypothesizing that ECV and GLS represent consistent markers of vulnerability.

METHODS

PATIENT POPULATION. This study complied with the Declaration of Helsinki, and the University of Pittsburgh Institutional Review Board approved the research protocol. Informed consent was obtained from all participants. We recruited 2,368 consecutive adult patients at time of clinical CMR at the UPMC

(14GRNT20380101) and a National Center for Advancing Translational Sciences of the NIH (KL2TR000146) grant. Dr. Schelbert was supported by a grant from The Pittsburgh Foundation (M2009-0068) and an American Heart Association Scientist Development grant (09SDG2180083) including a T. Franklin Williams Scholarship Award. Funding was provided by Atlantic Philanthropies, Inc., the John A. Hartford Foundation, the Association of Specialty Professors, and the American Heart Association. This work was also supported by grant UL1-TR-001857 from the National Center for Research Resources, a component of the NIH and the NIH Roadmap for Medical Research. Drs. Fröjdh, Maanja, Niklasson, Olausson, and Ugander were supported in part by grants (principal investigator: Dr. Ugander) from the Swedish Research Council, Swedish Heart and Lung Foundation, Stockholm County Council, and Karolinska Institutet. Dr. Butler is a consultant, speakerm, serves on steering committee, clinical events committee, and data safety monitoring for Abbott, Adrenomed, Amgen, Applied Therapeutics, Array, Astra Zeneca, Bayer, BerlinCures, Boehringer Ingelheim, Cardior, CVRx, Foundry, G3 Pharma, Imbria, Impulse Dynamics, Innolife, Janssen, LivaNova, Luitpold, Medtronic, Merck, Novartis, NovoNordisk, Relypsa, Roche, Sanofi, Sequana Medical, V-Wave Limited, and Vifor. Dr. Miller received research support from Roche and Guerbet; and is an advisory board participant for Novartis. Dr. Schelbert has accepted contrast material from Bracco Diagnostics for research purposes; served on advisory boards for Merck and Bayer; and currently serves on the Scientific Advisory Board of Haya Therapeutics. Dr. Ugander is principal investigator on a research and development agreement regarding cardiovascular magnetic resonance between Siemens and Karolinska University Hospital. Dr. Cavalcante has received consulting fees from Boston Scientific, Medtronic, and Abbott Vascular; and research grant support from Abbott Vascular, Edwards Lifesciences, Medtronic, Boston Scientific, Circle Cardiovascular Imaging, Siemens Healthineers, and Medis. All other authors have reported that they have no relationships relevant to the contents of this paper to disclose.

The authors attest they are in compliance with human studies committees and animal welfare regulations of the authors' institutions and Food and Drug Administration guidelines, including patient consent where appropriate. For more information, visit the *JACC: Cardiovascular Imaging* author instructions page.

Manuscript received September 17, 2019; revised manuscript received April 8, 2020, accepted April 9, 2020.

FIGURE 1 Study Cohort

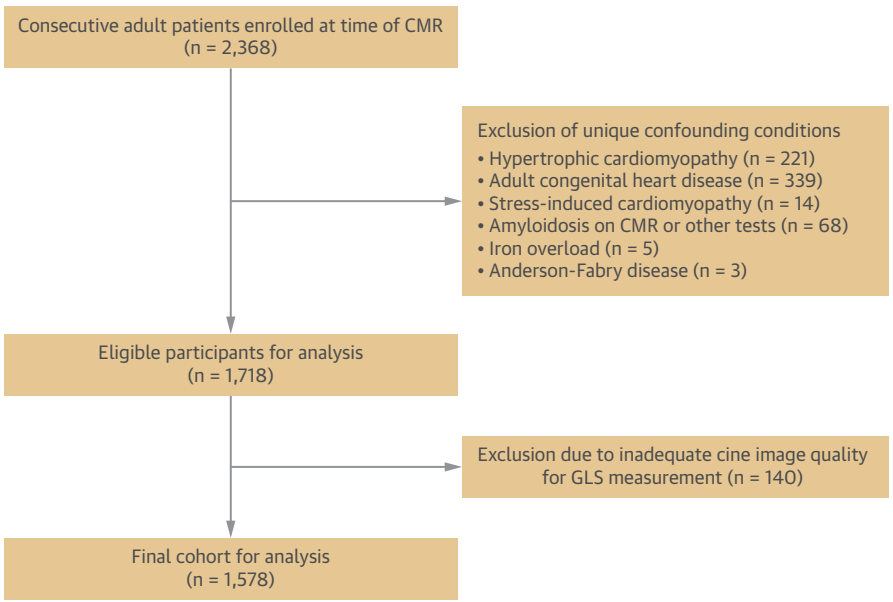

Flowchart describing the study cohort. CMR = cardiovascular magnetic resonance; GLS = global longitudinal strain.

Cardiovascular Magnetic Resonance Center from June 1, 2010, to March 31, 2016; they were followed up until October 11, 2018. The cohort was formed to examine a priori whether novel CMR measures of DMF associate with outcomes. Inclusion criteria were written informed consent and completion of a gadolinium contrast-enhanced CMR. Exclusion criteria included: 1) hypertrophic cardiomyopathy (n = 221), a unique genetic disorder; 2) adult congenital heart disease (n = 339); 3) any evidence at baseline CMR or during follow-up of marked interstitial expansion independent of collagen, namely myocardial edema due to stress-induced cardiomyopathy (n = 14) or interstitial expansion due to amyloid deposition in cardiac amyloidosis (n = 68) based on late gadolinium enhancement (LGE) patterns, ancillary clinical data at time of CMR scan, or any subsequent evidence of amyloidosis emerging during the follow-up period (e.g., biopsies or bone scintigraphy); 4) iron overload (n = 5) and Anderson-Fabry disease (n = 3); and 5) image quality inadequate to permit retrospective electrocardiography-gated segmented breath-held cine acquisition (n = 140). The final cohort for analysis included 1,578 participants (Figure 1).

DATA ELEMENTS. Data were managed by using REDCap (Research Electronic Data Capture), which incorporated quality checks such as missing data alerts, branching logic, and data range constraints to minimize data entry error (16). Baseline comorbidity data at the time of CMR were determined from the medical record. Patients were categorized according to heart failure stage defined by guidelines (25). First, HHF after CMR included any HHF event following CMR scanning (regardless of any prior HHF) and was identified by medical record review using a definition from previous epidemiological studies. HHF required physician documentation and the following: 1) documented symptoms and physical signs consistent with heart failure; 2) supporting clinical findings; or 3) therapy for heart failure. Vital status was ascertained by Social Security Death Index queries and medical record review.

CMR SCANS. **Cine CMR.** Patients underwent clinical CMR scans from a dedicated CMR center with a 1.5-T scanner (Magnetom Espree, Siemens Medical Solutions, Malvern, Pennsylvania) and a 32-channel phased-array cardiovascular coil. Examinations included standard cine imaging with 30 frames per cycle in long- and short-axis image planes with steady-state free precession as described previously (26). Typical parameters were: field of view, 380 × 320 cm; matrix, 256 × 144; 1.5 × 2.2 mm pixels; flip angle, 50°; temporal resolution, 30 to 50 ms; TR/TE = 2.9/1.2 ms; pixel bandwidth = 930 Hz; and parallel imaging factor 2 (generalized autocalibrating partially parallel acquisition). Left ventricular

TABLE 1 Baseline Characteristics of 1,578 Patients According to Whether GLS Was Above or Below the Median of -16.0% (Higher [Less Negative] Strain Values Equated With Worse Contractile Function)

	GLS -16.0% or Below (n = 791)	GLS -16.0% or Above (n = 787)	p Value
Demographic characteristics			
Age, yrs	53 (40–63)	59 (49–68)	<0.001
Female	431 (54.5)	250 (31.8)	<0.001
White race	709 (89.6)	677 (86.0)	0.028
Black race	62 (7.8)	90 (11.4)	0.015
Comorbidity			
Diabetes	105 (13.3)	210 (26.7)	<0.001
Hypertension	332 (42.0)	454 (57.7)	<0.001
Dyslipidemia	259 (32.7)	329 (41.8)	<0.001
Current cigarette smoking	85 (10.8)	145 (18.4)	<0.001
Previous cigarette smoking	214 (27.1)	254 (32.3)	0.023
Any atrial fibrillation or flutter	276 (34.9)	331 (42.6)	0.003
Hospitalized/inpatient status	182 (23.0)	374 (47.5)	<0.001
Previous coronary revascularization	74 (9.4)	205 (26.1)	<0.001
Previous percutaneous coronary intervention	49 (6.2)	153 (19.4)	<0.001
Previous coronary artery bypass grafting	32 (4.1)	90 (11.4)	<0.001
Moderate or severe aortic stenosis by echocardiography	12 (1.5)	22 (2.8)	0.080
Heart failure stage			
0	238 (30.1)	41 (5.2)	<0.001 for trend
A	348 (44.0)	117 (14.9)	
B	163 (20.6)	295 (37.5)	
C	42 (5.3)	334 (42.2)	
Body mass index, kg/m^2	28.1 (24.4–33.2)	29.0 (25.0–34.4)	0.026
General indication for CMR examination*			
Known or suspected cardiomyopathy	372 (47.0)	431 (54.8)	0.002
Possible coronary disease/viability/ vasodilator stress testing	272 (34.4)	414 (52.6)	<0.001
Vasodilator stress testing	188 (23.8)	222 (28.2)	0.044
Viability assessment	84 (10.6)	192 (24.4)	<0.001
Evaluation for arrhythmia substrate*	294 (37.2)	218 (27.7)	<0.001
Post-cardiac arrest evaluation	1 (0.1)	13 (1.7)	<0.001
Rule out ARVD evaluation	38 (4.8)	9 (1.1)	<0.001
Atrial fibrillation or flutter evaluation	66 (8.3)	89 (11.3)	0.048
Syncope	60 (7.6)	28 (3.6)	<0.001
Ventricular ectopy	29 (3.7)	14 (1.8)	0.021
Palpitations	112 (14.2)	68 (8.6)	<0.001
Sarcoidosis	50 (6.3)	22 (2.8)	<0.001
Valve disease assessment	70 (8.9)	49 (6.2)	0.049
Pericardial disease assessment	42 (5.3)	22 (2.8)	0.011
Possible mass or thrombus	31 (3.9)	47 (6.0)	0.060
Thoracic aorta assessment	34 (4.3)	19 (2.4)	0.038
Medications			
ACE inhibitor, angiotensin receptor blocker, or mineralocorticoid antagonist	242 (30.6)	443 (56.3)	<0.001
Beta-blockers	292 (36.9)	501 (63.7)	<0.001
Aspirin or other antiplatelet	330 (41.7)	457 (58.0)	<0.001
Statin	253 (32.0)	354 (45.0)	<0.001
Loop diuretic	98 (12.4)	248 (31.5)	<0.001
Non-loop diuretic	68 (8.6)	76 (9.7)	0.465

Continued on the next page

volumes and LVEF were measured without geometric assumptions from short-axis stacks of cines (6-mm thick, 4-mm space) by experienced readers. Right ventricular systolic dysfunction and right ventricular enlargement were expressed as ordinal variables with numeric values assigned to the degree of abnormality where 1 = normal, 2 = mild, 3 = moderate, and 4 = severe.

Global longitudinal strain. We used the semi-automated feature tracking analysis in Circle cvi[42] software (Circle Cardiovascular Imaging Inc., Calgary, Alberta, Canada) for GLS analysis blinded to outcome (6). Left ventricular epicardial and endocardial borders were manually traced in the 2-, 3-, and 4-chamber views at end-diastole, which were then propagated throughout the cardiac cycle. Automatic feature tracking yielded GLS measures. All contour tracings were inspected to ensure fidelity with manual adjustments as necessary. GLS measures included at least 2 long-axis images for strain assessment and were expressed as a percentage in which higher (less negative) values indicated worse contractile function. GLS measurement occurred blinded to comorbidity and outcome. For reference range purposes, 12 healthy control subjects (8 men and 4 women) with a median age of 23 years (range 18 to 30 years) were studied to identify -17.8% as the median and -15.5% as the upper 95% percentile threshold for GLS.

Late gadolinium enhancement. LGE imaging was performed 10 min after administration of a 0.2 mmol/kg intravenous gadoteridol bolus (ProHance, Bracco Diagnostics, Princeton, New Jersey) with phase-sensitive inversion recovery reconstruction. Image acquisition used segmented gradient echo and free breathing motion, steady-state free precession motion-corrected, phase-sensitive inversion recovery for LGE in the same image planes used for cine images (26). MI was identified when LGE involved the subendocardium in a typical coronary distribution. The semi-quantitative extent of MI and nonischemic LGE was assessed visually in terms of the extent of LGE (none, <25%, 26% to 50%, 51% to 75%, >75%); we assigned the midpoint value for each category (e.g., 12.5% for the <25% category) for each of the 17 segments and thus created 85 potential levels of global left ventricular involvement (16). Extent of involvement was expressed as a percentage of left ventricular mass.

QUANTIFICATION OF DMF. Reproducible (27) and validated (2,3) Modified Look-Locker inversion recovery sequences were used to measure ECV in noninfarcted myocardium, as previously described (Supplemental Methods) (15). To focus on DMF, we

also excluded from ECV measures any myocardium demonstrating LGE from any etiology or near any potential area at risk. ECV was measured in the middle third of myocardium, and the myocardium-blood pool interface was meticulously avoided to avoid partial volume effects.

DMF was quantified, with ECV defined as: ECV = λ (1 − hematocrit) where $\lambda = [\Delta R1_{myocardium}]/[\Delta R1_{bloodpool}]$ before and after gadolinium contrast administration (where R1 = 1/T1) (1). Each T1 and ECV measurement for a short-axis slice location was derived from a single native and post-contrast T1 map occurring following acquisition of clinical LGE images (usually 15 to 20 min after contrast bolus). Hematocrit values were acquired on the day of scanning (from the intravenous cannula in outpatients or from routine measures in hospitalized patients) and measured in the clinical laboratory. We averaged ECV values from basal and mid-ventricular short-axis slices to yield final measurements. Apical slices were excluded due to error concerns related to partial volume averaging. ECV measures were expressed as a percentage and occurred blinded to GLS and outcome. We previously identified ECV measures of 28.5% in healthy volunteers as the upper limit of normal (16).

TABLE 1 Continued

	GLS −16.0% or Below (n = 791)	GLS −16.0% or Above (n = 787)	p Value
Laboratory and CMR characteristics			
ECV, %	27.0 (24.8–29.4)	27.9 (25.5–31.0)	<0.001
Creatinine, mg/dl	0.9 (0.8–1.1)	1.0 (0.8–1.2)	<0.001
Glomerular filtration rate, ml/min/1.73 m^2	90 (77–103)	82 (66–95)	<0.001
Hematocrit, %	39.0 (35.9–41.9)	39.0 (35.0–42.8)	0.783
Ejection fraction, %	63 (59–67)	45 (32–56)	<0.001
LV mass index, g/m^2	48 (41–60)	66 (54–81)	<0.001
End-diastolic volume index, ml/m^2	74 (64–87)	96 (75–120)	<0.001
End-systolic volume index, ml/m^2	27 (21–34)	52 (34–79)	<0.001
Moderate or severe mitral regurgitation by cine CMR	13 (1.6)	49 (6.2)	<0.001
Any LGE	139 (17.6)	466 (59.2)	<0.001
MI by LGE	54 (6.8)	291 (37.0)	<0.001
Infarct size, % LV mass, among those with MI	3.7 (1.5–8.1)	17.6 (7.4–27.9)	<0.001
Nonischemic scar by LGE	92 (11.6)	198 (25.4)	<0.001
Nonischemic scar, % LV mass, among those with evident scar on LGE	2.1 (0.7–3.6)	3.3 (1.5–7.2)	<0.001

Values are median (quartile 1-quartile 3) or n (%), unless otherwise indicated. *The categories for cardiovascular magnetic resonance (CMR) indication were not exclusive. Thus, patients could have multiple indications for CMR, and there may be overlap in the classification of indication(s).

ACE = angiotensin-converting enzyme; ARVD = arrhythmogenic right ventricular dysplasia; ECV = extracellular volume; GLS = global longitudinal strain; LGE = late gadolinium enhancement; LV = left ventricular; MI = myocardial infarction.

STATISTICAL ANALYSIS. Categorical variables were summarized with numbers (percentages). We summarized continuous variables with median (interquartile range) because some variables exhibited skewed non-normal distributions based on the Kolmogorov-Smirnov test. Chi-square tests were used to compare categorical variables between patients; similarly, Wilcoxon rank sum tests compared continuous variables. Baseline variables were compared according to whether GLS was above or below the median.

Univariable and multivariable linear regression was used to evaluate how ECV and other variables associated with GLS. We elected to use stepwise selection to identify variables associated with GLS in multivariable linear regression models where variable inflation factors <2 reasonably excluded significant collinearity. The t values exhibited strength of association, and R^2 values expressed how much the variables explained the variation in GLS.

Survival analyses examined a combined endpoint of time to either first HHF or death (all-cause mortality) (16). Kaplan-Meier curves used the log-rank test dividing ECV and GLS into 5 equally spaced strata with 1 SD intervals (2 strata below and 3 strata above the median). We preferred this approach over one using quantiles because the clinician wishes to estimate risk with progressive deviation from normal, regardless of whether strata contain equal numbers of patients. Regardless, univariable and multivariable Cox regression models ultimately quantified associations between variables and outcomes, whereby chi-square values tested the strength of these associations and permitted benchmark comparisons between GLS, ECV, and other variables within the model. We confirmed the proportional hazards assumption for GLS and ECV variables by nonsignificant interactions with time. We modeled continuous variables as such but scaled the hazard ratios (HRs) to 1 SD intervals for comparison purposes, which did not affect resultant chi-square or p values.

A primary multivariable Cox model was created adjusting for clinical variables stratifying according to hospitalization status (i.e., inpatient), which is a nonspecific summary marker of frailty. A secondary Cox model was created further stratifying according to heart failure stage to investigate whether associations between covariates and outcome change after further adjustment for a nonspecific summary measure that likely reflects downstream measures of intrinsic myocardial disease such as GLS and ECV. Finally, univariable and multivariable Cox regression

FIGURE 2 Ejection Fraction and GLS Exhibit Strong Linear Correlation But ECV and GLS Only Correlate Minimally

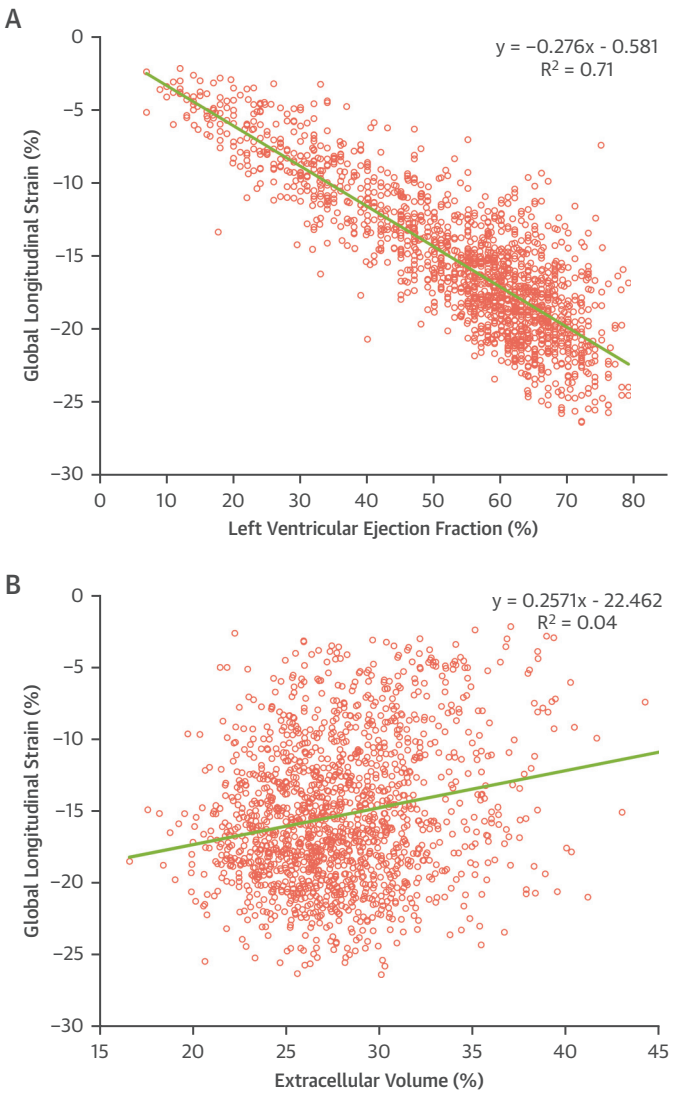

(A) Global longitudinal strain (GLS) and left ventricular ejection fraction exhibit a close linear relationship across the spectrum of ejection fraction. **(B)** In contrast, GLS exhibited minimal correlation with extracellular volume (ECV) measures of questionable clinical significance.

analyses were repeated to examine clinically important subgroups. All multivariable linear and Cox regression models used stepwise selection based on a p value ≤0.1 to enter and remain in the model.

As described previously (21), we used integrated discrimination improvement (IDI) and net reclassification improvement (NRI) indices to evaluate the added predictive ability of univariable and multivariable Cox regression models with ECV versus Cox regression models without ECV (Supplemental Methods). Statistical tests were two sided, and $p < 0.05$ was considered significant. Statistical analyses were performed by using SAS version 9.4 (SAS Institute, Inc., Cary, North Carolina).

RESULTS

BASELINE CHARACTERISTICS. GLS ranged from -26.4% to -2.17%, with a median of -16.0% (quartile 1 to quartile 3 [Q1 to Q3]: -18.8% to -12.1%). ECV ranged from 16.6% to 46.9%, with a median of 27.5% (Q1 to Q3: 25.1% to 30.3%). Table 1 summarizes patients' baseline characteristics according to whether GLS was above the median, indicating worse contractile function. Those with higher GLS were older, were more often male, and exhibited higher comorbidity with lower LVEF, higher left ventricular mass and volumes, and slightly higher ECV measures of DMF.

Variables associated with higher GLS. Supplemental Table 1 presents the variables associated with GLS in univariable and multivariable linear regression models. Supplemental Table 2 limited covariates to CMR variables only and yielded an R^2 magnitude similar to that in Supplemental Table 1 (0.749 vs. 0.779). LVEF clearly exhibited the strongest (inverse) association with GLS and explained 71% of its variation (R^2) in a univariable model. GLS and LVEF exhibited a linear relationship across the spectrum of LVEF (Figure 2).

In contrast, GLS and ECV were minimally related with an R^2 of only 0.04 (Figure 2). Higher left ventricular mass also associated with higher (worse) GLS (Supplemental Tables 1 and 2). The Supplemental GLS Results provide additional analyses of factors associated with GLS.

Comparing GLS and ECV in their associations with outcomes. Over a median follow-up of 5.6 years (Q1 to Q3: 4.1 to 6.6 years), 339 patients experienced adverse events (149 HHF, 253 deaths, and 63 experiencing both). Despite weak correlations between ECV and GLS, both GLS and ECV each associated strongly with incident outcomes, including HHF, death, or both (Figure 3). As GLS or ECV increased, risks of adverse events also increased, with both GLS and ECV exhibiting dose-response relationships in survival analysis curves. Those with both ECV and GLS above the median reported the highest event rates (Figure 4).

Similar patterns emerged in Cox regression models expressing ECV and GLS as continuous variables. Both ECV and GLS exhibited strong associations with outcomes (i.e., death or HHF) in univariable models and multivariable models using stepwise selection to

FIGURE 3 **GLS and ECV Each Stratify Risk Robustly in a Dose-Response Fashion**

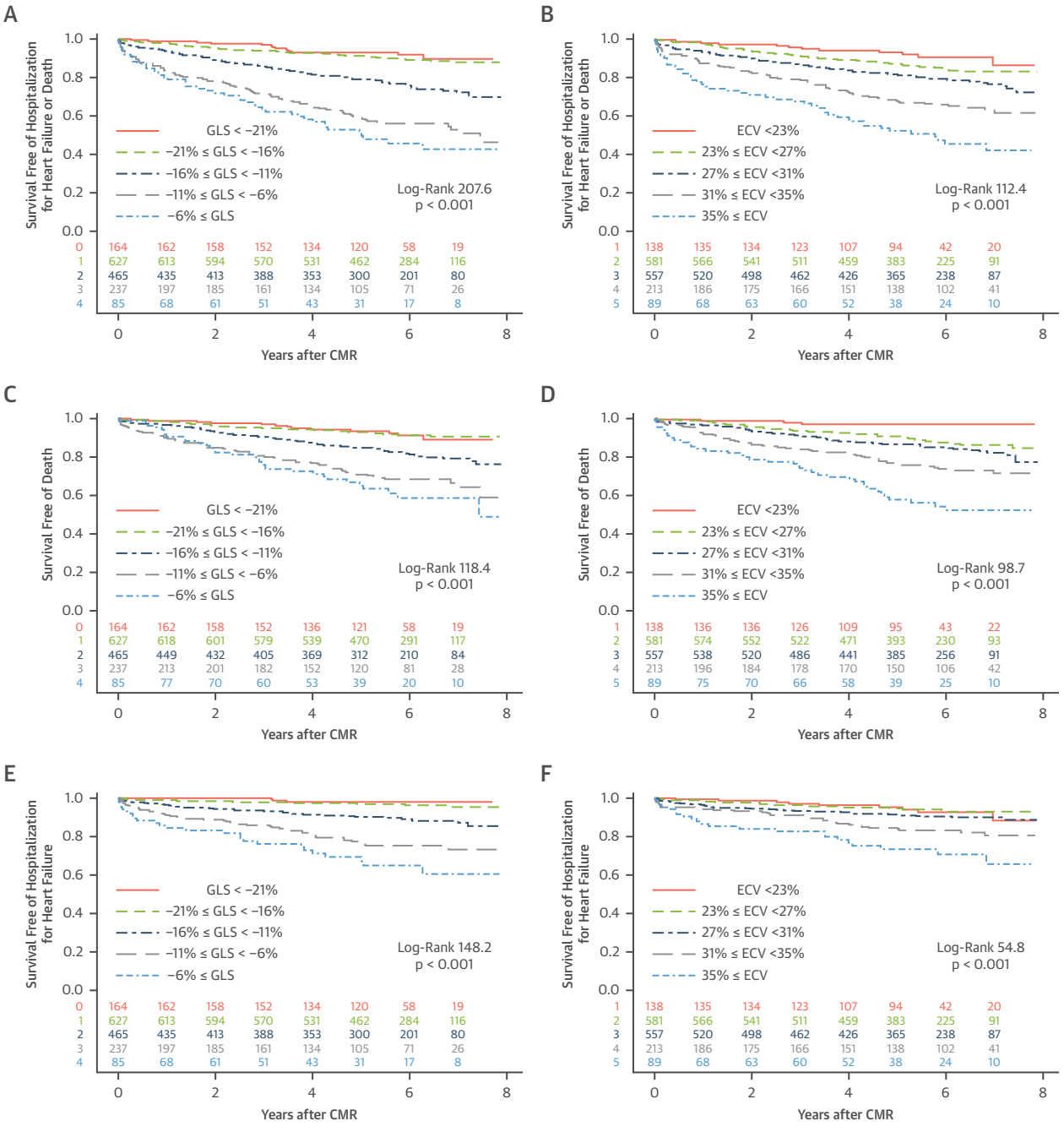

Stratifying the sample (N = 1,578) according to GLS **(A, C, E)** or ECV **(B, D, F)** with SD increments revealed robust associations with the outcomes of: 1) either hospitalization for heart failure or death (n = 339; **A and B**); 2) all-cause death (n = 253; **C and D**); or 3) hospitalization for heart failure only censoring for death (n = 149; **E and F**). Abbreviations as in Figures 1 and 2.

adjust for various comorbidities, as specified in Table 2. Cox regression analyses identified ECV and GLS as principal imaging biomarkers in which elevations indicate patient vulnerability to adverse outcomes. Other variables related to associated comorbidity (e.g., diabetes, hypertension, MI, coronary artery disease, smoking, renal disease), LGE, or left ventricular mass exhibited weaker associations.

FIGURE 4 Highest Event Rates Experienced by Patients With Both Elevated ECV and GLS

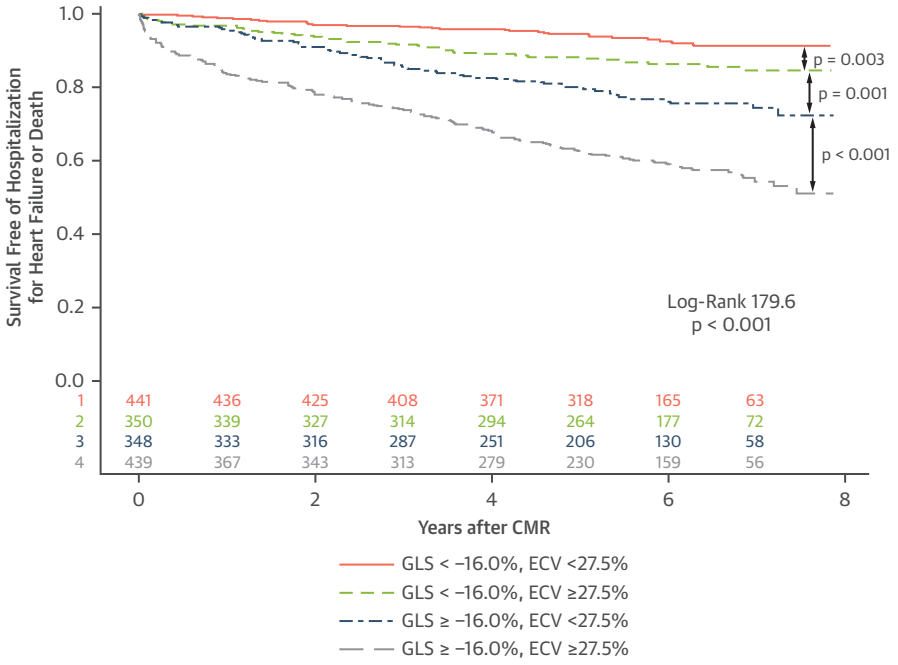

When separating the sample into 4 crude categories according to whether ECV and GLS were simply above or below the median, those with both elevated ECV and GLS experienced the highest incidence of death or heart failure, suggesting additive effects of combined diffuse fibrosis and contractile dysfunction. (The p values between strata do not adjust for multiple comparisons). Abbreviations as in Figures 1 and 2.

Importantly, other metrics of myocardial disease such as left ventricular mass, MI, and nonischemic scar did not significantly associate with outcomes in multivariable models. Further adjustment for heart failure stage, which associates with GLS, weakened the associations between GLS and outcomes more so than ECV. ECV and GLS did not interact significantly ($p = 0.992$), indicating that risks for 1 variable did not vary as a function of the other. GLS exhibited stronger associations with outcomes than LVEF. When only GLS and LVEF were included in a Cox regression model, GLS remained associated with outcomes ($p < 0.001$) but LVEF did not ($p = 0.269$). Therefore, GLS was the preferred metric of contractile dysfunction for subsequent models. Adding LVEF to the pool of covariates did not change any of the stepwise selection models. Ordinal variables related to right ventricular systolic dysfunction and right ventricular enlargement both associated with outcomes in univariable models ($p < 0.001$ for both) but not in fully adjusted stepwise multivariable models ($p > 0.10$ for both).

Examining components of the combined endpoint, ECV and GLS associated with incident all-cause mortality in stepwise multivariable models (HR 1.51 per 4% ECV increment [95% CI: 1.37 to 1.71; chi-square: 43.1; $p < 0.001$] and HR 1.34 per 5% GLS increment [95% CI: 1.17 to 1.55; chi-square: 17.0; $p < 0.001$], respectively), but age yielded the highest chi-square value of 58.4. Similarly, ECV and GLS associated with incident HHF (censoring for death) in stepwise multivariable models (HR 1.31 per 4% ECV increment [95% CI: 1.12 to 1.53; chi-square: 11.4; $p < 0.001$] and HR 1.79 per 5% GLS increment [95% CI: 1.50 to 2.14; chi-square: 40.4; $p < 0.001$]), where GLS yielded the highest chi-square value.

ECV added prognostic value when added to a univariable Cox model containing GLS, yielding significant IDI and NRI statistics (IDI = 0.007 [95% CI: 0.005 to 0.011; $p < 0.001$]; $NRI_{continuous} = 0.256$ [95% CI: 0.138 to 0.368; $p < 0.001$]; $NRI_{categorical} = 0.122$ [95% CI: 0.081 to 0.168; $p < 0.001$]). ECV also added prognostic value when added to a fully adjusted multivariable Cox regression model (without stepwise selection) and still yielded significant IDI and NRI statistics (IDI = 0.006 [95% CI: 0.001 to 0.013; $p = 0.02$]; $NRI_{continuous} = 0.234$ [95% CI: 0.115 to 0.377; $p = 0.001$]; $NRI_{categorical} = 0.034$ [95% CI: 0.026 to 0.080; $p = 0.020$]).

CENTRAL ILLUSTRATION **Global Longitudinal Strain and Extracellular Volume May Represent Principal But Distinct Domains of Cardiac Vulnerability**

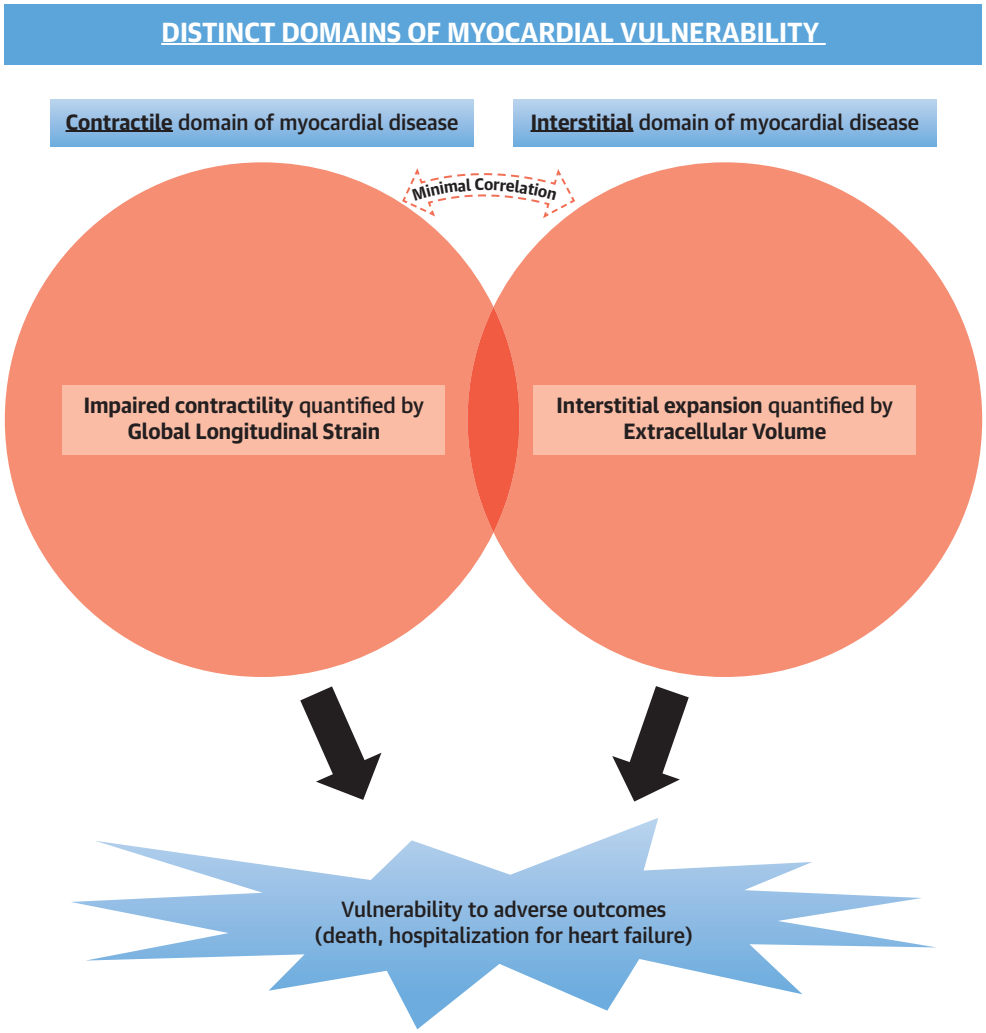

Fröjdh, F. et al. J Am Coll Cardiol Img. 2020;■(■):■-■.

Among myriad changes occurring in diseased myocardium, assessment of myocardial interstitial and contractile domains may provide a classification scheme to conceptualize vulnerability to adverse events, as global longitudinal strain and extracellular volume represent principal but distinct domains of cardiac vulnerability.

Subgroup analyses. In subgroup analyses (Supplemental Table 3), both GLS and ECV remained significantly associated with outcomes in univariable and stepwise multivariable Cox models examining patients with: preserved or reduced LVEF <55%; heart failure with reduced LVEF; MI according to LGE, present or absent; clinical diagnosis of diabetes, present or absent; and any clinical evidence of coronary disease, present or absent. In the small subset of cases of heart failure with preserved LVEF, GLS did not significantly associate with outcomes but ECV did.

In the 1,398 patients (89%) with available B-type natriuretic peptide (BNP) levels measured on the day of CMR scanning, ECV and GLS remained associated with outcomes (n = 306) in the fully adjusted stepwise multivariable model, stratifying according to hospitalization and even heart failure stage and further adjusting for log-transformed BNP (HR: 1.24 per 4% ECV increment [95% CI: 1.10 to 1.39;

TABLE 2 Univariable and Stepwise Multivariable Cox Regression Models for Outcomes of Either Death or Hospitalization for Heart Failure (n = 339) in the Entire Cohort (N = 1,578)

	Univariable Model			Multivariable Model Without Stratification for Heart Failure Stage			Multivariable Model With Stratification for Heart Failure Stage		
	Chi-Square Value	HR (95% CI)	p Value	Chi-Square Value	HR (95% CI)	p Value	Chi-Square Value	HR (95% CI)	p Value
GLS (per 5% increment)	188.7	2.07 (1.86–2.29)	<0.001	55.6	1.56 (1.39–1.76)	<0.001	25.1	1.42 (1.24–1.62)	<0.001
LVEF (per 15% decrement)	141.5	1.74 (1.59–1.91)	<0.001					–	
ECV (per 4% increment)	114.9	1.66 (1.51–1.82)	<0.001	36.3	1.39 (1.25–1.54)	<0.001	30.3	1.36 (1.22–1.52)	<0.001
Age (per 15-yr increment)	108.9	1.89 (1.68–2.13)	<0.001	28.5	1.46 (1.27–1.68)	<0.001	27.6	1.45 (1.26–1.67)	<0.001
LV mass index (per 21 g/m^2)	80.6	1.45 (1.34–1.57)	<0.001						
Diabetes mellitus, type 2	77.7	2.71 (2.17–3.37)	<0.001	12.8	1.54 (1.21–1.94)	<0.001	10.5	1.48 (1.17–1.87)	0.001
MI	69.3	2.53 (2.04–3.16)	<0.001						
Hypertension	62.5	2.54 (2.02–3.20)	<0.001	9.7	1.49 (1.16–1.92)	0.002	8.7	1.48 (1.14–1.92)	0.003
Glomerular filtration rate, (per 24 ml/min/1.73 m^2 decrement)	55.7	1.57 (1.40–1.77)	<0.001	5.6	1.15 (1.02–1.29)	0.018	3.2	1.11 (0.99–1.25)	0.073
Previous CABG	50.8	2.84 (2.13–3.78)	<0.001	4.1	1.37 (1.01–1.86)	0.042	3.3	1.33 (0.98–1.79)	0.068
Percentage of MI mass (per 9% increment)	49.8	1.30 (1.21–1.40)	<0.001					–	
End-diastolic volume index (per 33 ml/m^2)	48.8	1.34 (1.23–1.45)	<0.001						
Significant mitral regurgitation	28.1	2.80 (1.91–4.10)	<0.001						
Previous percutaneous coronary intervention	17.7	1.78 (1.36–2.32)	<0.001						
Nonischemic scar on LGE	16.3	1.67 (1.30–2.12)	<0.001						
Current cigarette smoking	13.6	1.64 (1.26–2.14)	<0.001	8.7	1.55 (1.16–2.08)	0.003	9.5	1.58 (1.18–2.12)	0.002
Atrial fibrillation	13.4	1.75 (1.30–2.36)	<0.001	4.5	1.39 (1.03–1.89)	0.033	4.6	1.40 (1.03–1.90)	0.032
Moderate or severe aortic stenosis	13.0	2.59 (1.54–4.35)	<0.001						
Nonischemic scar mass (per 3% increment)	12.3	1.16 (1.07–1.26)	<0.001					–	
Dyslipidemia	11.6	1.45 (1.17–1.80)	<0.001						
Previous cigarette smoking	10.1	1.43 (1.15–1.79)	0.002	4.8	1.31 (1.03–1.68)	0.028	4.4	1.30 (1.02–1.66)	0.036
White race	4.1	0.74 (0.55–0.99)	0.044	3.0	0.76 (56–1.04)	0.084			
Female	4.0	0.80 (0.64–1.00)	0.046						

The chi-square values permit comparisons of strength of associations with outcomes. Hazard ratios (HRs) were modeled as continuous variables but scaled to 1 SD increments (which does not affect p values or chi-square values). We created multivariable models stratified according to hospitalization status, and additional models were further stratified according to heart failure stage, a variable strongly associated with GLS (Supplemental Table 2).

CABG = coronary artery bypass grafting; CI = confidence interval; LVEF = left ventricular ejection fraction; other abbreviations as in Table 1.

chi-square: 12.0; $p < 0.001$]; HR 1.25 per 5% GLS increment [95% CI: 1.07 to 1.45; chi-square: 8.4; $p = 0.004$]). The model ignored potential collinear relationships between covariates (in which abnormal ECV and/or GLS culminate in increased BNP).

DISCUSSION

Among myriad changes occurring in diseased myocardium, the myocardial interstitium and contractile function may represent principal domains of myocardial disease that remain largely independent of one another (**Central Illustration**). ECV, possibly indicating architectural distortion most often from DMF mediated by fibroblasts (2), and GLS, possibly indicating cardiomyocyte contractile dysfunction, each may capture fundamental myocardial derangements originating from distinct cell types. Each metric robustly associated with outcomes (HHF, death, or both) in a dose-response fashion with progressively divergent survival curves. However, GLS and ECV only correlated weakly, and therefore one was not a proxy for the other. In contrast, LVEF and GLS correlated highly. Because GLS associated more strongly with outcomes than LVEF, GLS may represent a better contractile measure of risk. Other variables related to associated comorbidity (e.g., diabetes, coronary disease) or specific myocardial disease phenotypes (e.g., left ventricular mass, MI, nonischemic scar) did not exhibit strong associations with outcomes.

Measuring both contractile and interstitial domains of cardiac vulnerability may: 1) provide more complete myocardial phenotyping that captures pathophysiology probably originating from distinct cell types; 2) improve risk stratification; and 3) foster personalized precision medicine through specific therapeutics targeting the affected domain(s). DMF diagnosed by ECV might indicate potential eligibility for therapy targeting collagen metabolism and/or fibroblast/myofibroblast function (19,28,29). Alternatively, contractile dysfunction diagnosed by GLS may

indicate potential eligibility for therapy targeting the cardiomyocyte, which could include calcium handling, mitochondrial energetics, or other substrates (30,31). Further research should investigate these issues.

The slow progress in reversing adverse heart failure trends over the past 2 decades underscores the complexities of reversing myocardial disease. We propose that future Phase II heart failure trials include GLS and ECV assessments to quantify how principal interstitial and contractile domains of cardiac vulnerability respond to therapeutic interventions (29). The cardiology community ultimately requires Phase III trials to show that GLS and/or ECV directed therapies improve outcomes.

Results of the current analyses agree with previous published reports. We affirm prior associations between CMR GLS and mortality in the setting of dilated cardiomyopathy or reduced LVEF (6-8) and extend associations to include the full spectrum of LVEF (6), even while accounting for ECV, a powerful predictor of events (16,20,21). Furthermore, we illustrate that GLS and ECV each might potentially reflect principal contractile and interstitial domains of patient vulnerability, respectively, across the spectrum of LVEF that seem distinct from one other. Others have published NRI data for GLS (7), and the current study furnishes NRI/IDI data for ECV beyond GLS and other covariates. Beyond mortality, we also show, for both GLS and ECV, robust dose-response associations with incident HHF (i.e., censoring for death), an important event among surviving patients. Finally, the positive correlations between left ventricular mass and GLS suggest hypertrophy as a potential compensatory mechanism in response to abnormally increased GLS (23).

STUDY LIMITATIONS. First, observational data do not establish causality and may generate associations from residual uncontrolled confounding. For example, we did not have right ventricular and left atrial volumetric data. To minimize confounding, we attempted robust risk adjustment in a large dataset with multiple modeling strategies across many subgroups. Second, single-center data with inherent referral biases affecting prevalence of competing comorbidity may not generalize. ECV measures might vary according to pulse sequence, contrast agent, and field strength. However, our cohort from an integrated health system reflecting our practice is among the largest reported to date, and results align with prior literature. Third, our data may not extend to those with arrhythmia or who cannot breath-hold to generate segmented cines. Novel pulse sequence development could remedy this problem as CMR technology continues to develop. Fourth, medical record review may yield imperfect event adjudication. However, adjudication errors would bias toward the null hypothesis.

CONCLUSIONS

Among myriad changes occurring in diseased myocardium, contractile metrics such as GLS (potentially reflecting cardiomyocyte contractile dysfunction) and interstitial metrics such as ECV (potentially reflecting fibroblast dysfunction) may represent principal metrics of vulnerability to adverse outcomes across the spectrum of LVEF, extending to several clinically important subgroups. Because GLS and ECV correlate minimally, they are not proxies for one other. The cardiology community requires further investigation to determine whether combining both contractile and interstitial metrics may optimize pathophysiologic understanding, optimize risk stratification through more comprehensive assessment of cardiac disease, and foster personalized precision medicine by targeted therapeutics.

ADDRESS FOR CORRESPONDENCE: Dr. Erik B. Schelbert, University of Pittsburgh School of Medicine, 200 Lothrop Street, PUH E E354.2, Pittsburgh, Pennsylvania 15101. E-mail: schelberteb@upmc.edu. Twitter: @erik_schelbert.

PERSPECTIVES

COMPETENCY IN MEDICAL KNOWLEDGE: ECV and GLS may represent principal but distinct domains of cardiac vulnerability. GLS and ECV correlate minimally with one another, yet both ECV and GLS associate robustly with incident outcomes (HHF, death, or both) in a large cohort (N = 1,578). These associations extend to various clinically important subgroups.

TRANSLATIONAL OUTLOOK: The cardiology community requires further investigation to determine whether combining both contractile and interstitial metrics may optimize pathophysiological understanding for a given patient, optimize risk stratification through more comprehensive assessment of cardiac disease, and foster personalized precision medicine by targeted therapeutics.

REFERENCES

1. Messroghli DR, Moon JC, Ferreira VM, et al. Clinical recommendations for cardiovascular magnetic resonance mapping of T1, T2, T2* and extracellular volume: a consensus statement by the Society for Cardiovascular Magnetic Resonance (SCMR) endorsed by the European Association for Cardiovascular Imaging (EACVI). J Cardiovasc Magn Reson 2017;19:75.

2. Schelbert EB, Sabbah HN, Butler J, Gheorghiade M. Employing extracellular volume cardiovascular magnetic resonance measures of myocardial fibrosis to foster novel therapeutics. Circ Cardiovasc Imaging 2017;10:e005619.

3. Miller CA, Naish J, Bishop P, et al. Comprehensive validation of cardiovascular magnetic resonance techniques for the assessment of myocardial extracellular volume. Circ Cardiovasc Imaging 2013;6:373–83.

4. Pedrizzetti G, Claus P, Kilner PJ, Nagel E. Principles of cardiovascular magnetic resonance feature tracking and echocardiographic speckle tracking for informed clinical use. J Cardiovasc Magn Reson 2016;18:51.

5. Schuster A, Hor KN, Kowallick JT, Beerbaum P, Kutty S. Cardiovascular magnetic resonance myocardial feature tracking: concepts and clinical applications. Circ Cardiovasc Imaging 2016;9:e004077.

6. Kammerlander AA, Kraiger JA, Nitsche C, et al. Global longitudinal strain by CMR feature tracking is associated with outcome in HFPEF. J Am Coll Cardiol Img 2019;12:1585–7.

7. Romano S, Judd RM, Kim RJ, et al. Feature-tracking global longitudinal strain predicts death in a multicenter population of patients with ischemic and nonischemic dilated cardiomyopathy incremental to ejection fraction and late gadolinium enhancement. J Am Coll Cardiol Img 2018;11:1419–29.

8. Buss SJ, Breuninger K, Lehrke S, et al. Assessment of myocardial deformation with cardiac magnetic resonance strain imaging improves risk stratification in patients with dilated cardiomyopathy. Eur Heart J Cardiovasc Imaging 2015;16:307–15.

9. Lurz JA, Luecke C, Lang D, et al. CMR-derived extracellular volume fraction as a marker for myocardial fibrosis: the importance of coexisting myocardial inflammation. J Am Coll Cardiol Img 2018;11:38–45.

10. Ugander M, Oki AJ, Hsu LY, et al. Extracellular volume imaging by magnetic resonance imaging provides insights into overt and sub-clinical myocardial pathology. Eur Heart J 2012;33:1268–78.

11. Rommel KP, von Roeder M, Latuscynski K, et al. Extracellular volume fraction for characterization of patients with heart failure and preserved ejection fraction. J Am Coll Cardiol 2016;67:1815–25.

12. Mordi IR, Singh S, Rudd A, et al. Comprehensive echocardiographic and cardiac magnetic resonance evaluation differentiates among heart failure with preserved ejection fraction patients, hypertensive patients, and healthy control subjects [published correction appears in J Am Coll Cardiol Img 2019;12:576]. J Am Coll Cardiol Img 2018;11:577–85.

13. Mohammed SF, Hussain S, Mirzoyev SA, Edwards WD, Maleszewski JJ, Redfield MM. Coronary microvascular rarefaction and myocardial fibrosis in heart failure with preserved ejection fraction. Circulation 2015;131:550–9.

14. Tamarappoo BK, John BT, Reinier K, et al. Vulnerable myocardial interstitium in patients with isolated left ventricular hypertrophy and sudden cardiac death: a postmortem histological evaluation. J Am Heart Assoc 2012;1:e001511.

15. Wong TC, Piehler K, Meier CG, et al. Association between extracellular matrix expansion quantified by cardiovascular magnetic resonance and short-term mortality. Circulation 2012;126:1206–16.

16. Schelbert EB, Piehler KM, Zareba KM, et al. Myocardial fibrosis quantified by extracellular volume is associated with subsequent hospitalization for heart failure, death, or both across the spectrum of ejection fraction and heart failure stage. J Am Heart Assoc 2015;4:e002613.

17. Chin CW, Everett RJ, Kwiecinski J, et al. Myocardial fibrosis and cardiac decompensation in aortic stenosis. J Am Coll Cardiol Img 2016;10:1320–33.

18. Kammerlander AA, Marzluf BA, Zotter-Tufaro C, et al. T1 mapping by CMR imaging: from histological validation to clinical implication. J Am Coll Cardiol Img 2016;9:14–23.

19. Schelbert EB, Fridman Y, Wong TC, et al. Temporal relation between myocardial fibrosis and heart failure with preserved ejection fraction: association with baseline disease severity and subsequent outcome. JAMA Cardiol 2017;2:1–12.

20. Yang EY, Ghosn MG, Khan MA, et al. Myocardial extracellular volume fraction adds prognostic information beyond myocardial replacement fibrosis. Circ Cardiovasc Imaging 2019;12:e009535.

21. Treibel TA, Fridman Y, Bering P, et al. Extracellular volume associates with outcomes more strongly than native or post-contrast myocardial T1. J Am Coll Cardiol Img 2020;13:44–54.

22. Russo C, Jin Z, Elkind MS, et al. Prevalence and prognostic value of subclinical left ventricular systolic dysfunction by global longitudinal strain in a community-based cohort. Eur J Heart Fail 2014;16:1301–9.

23. Stokke TM, Hasselberg NE, Smedsrud MK, et al. Geometry as a confounder when assessing ventricular systolic function: comparison between ejection fraction and strain. J Am Coll Cardiol 2017;70:942–54.

24. Li R, Yang ZG, Xu HY, et al. Myocardial deformation in cardiac amyloid light-chain amyloidosis: assessed with 3T cardiovascular magnetic resonance feature tracking. Sci Rep 2017;7:3794.

25. Hunt SA, Abraham WT, Chin MH, et al. 2009 Focused update incorporated into the ACC/AHA 2005 Guidelines for the Diagnosis and Management of Heart Failure in Adults A Report of the American College of Cardiology Foundation/American Heart Association Task Force on Practice Guidelines Developed in Collaboration With the International Society for Heart and Lung Transplantation. J Am Coll Cardiol 2009;53:e1–90.

26. Piehler KM, Wong TC, Puntil KS, et al. Free-breathing, motion-corrected late gadolinium enhancement is robust and extends risk stratification to vulnerable patients. Circ Cardiovasc Imaging 2013;6:423–32.

27. Schelbert EB, Testa SM, Meier CG, et al. Myocardial extravascular extracellular volume fraction measurement by gadolinium cardiovascular magnetic resonance in humans: slow infusion versus bolus. J Cardiovasc Magn Reson 2011;13:16.

28. Micheletti R, Plaisance I, Abraham BJ, et al. The long noncoding RNA Wisper controls cardiac fibrosis and remodeling. Sci Transl Med 2017;9.

29. González A, Schelbert EB, Diez J, Butler J. Myocardial interstitial fibrosis in heart failure, biological and translational perspectives. J Am Coll Cardiol 2018;71:1696–706.

30. Lewis GA, Schelbert EB, Williams SG, et al. Biological phenotypes of heart failure with preserved ejection fraction. J Am Coll Cardiol 2017;70:2186–200.

31. Brown DA, Perry JB, Allen ME, et al. Expert consensus document: mitochondrial function as a therapeutic target in heart failure. Nat Rev Cardiol 2017;14:238–50.

KEY WORDS cardiac magnetic resonance, extracellular volume, global longitudinal strain, interstitium, myocardial fibrosis

APPENDIX For supplemental Methods, Results, and tables, please see the online version of this paper.